Omnidirectional magnetic-resonance transmission and its elimination in a metallic metamaterial comprising rings and plates

Zheng-Gao Dong,[1,*] Ming-Xiang Xu,[1] Hui Liu,[2] Tao Li,[2] and Shi-Ning Zhu[2]
[1]*Physics Department, Southeast University, Nanjing 211189, People's Republic of China*
[2]*National Laboratory of Solid State Microstructures, Nanjing University, Nanjing 210093, People's Republic of China*
(Received 19 August 2008; revised manuscript received 27 October 2008; published 31 December 2008)

Magnetic resonance is numerically investigated in a metallic metamaterial comprising rings and plates. It is found that a transmission band, instead of a stop band, results from the magnetic resonance as long as the electric field of the incident wave is polarized parallel to the ring plane, and thus it is an omnidirectional magnetic resonance transmission. We also observe an elimination phenomenon of the magnetic resonance transmission by tailoring the size of the plate, which implies a magnitude modulation of magnetic resonance. In addition, the equivalent *LC* circuit model is applied to analyze the geometry dependence of the magnetic resonance frequency, which is consistent with the numerical results by parametric simulations on the structural variations.

DOI: 10.1103/PhysRevE.78.066612 PACS number(s): 41.20.Jb, 42.70.Qs, 78.20.Ci, 73.20.Mf

I. INTRODUCTION

Resonant metamaterial with metallic elements in subwavelength sizes creates an artificial access to many electromagnetic behaviors that were previously unavailable by naturally occurring materials, such as the superimaging [1], negative refraction [2], and cloaking phenomenon [3]. One of the common issues shared by these electromagnetic effects is the magnetic activity at gigahertz frequencies and above [4–6]. Generally, such artificial magnetism is obtained through resonance and can be described by the equivalent *LC* circuit model with the resonance frequency written as $f_0=1/(2\pi\sqrt{L_{\mathrm{eff}}C_{\mathrm{eff}}})$, where the effective inductance L_{eff} is attributed to the induced circulating or antiparallel current distributions, and the effective capacitance C_{eff} is formed by accumulated charges between the front and end of the excited conduction currents [7–9].

As for the *LC*-resonance magnetic metamaterials, one of the disadvantages is that a large portion of them, such as the split-ring [10], H-shaped [11], and U-shaped [12] structures, respond magnetically only if the wave vector of the electromagnetic field is in a lateral propagation direction with respect to the planar metallic element. On the other hand, although the fishnet [13–15] and rod-pair [16,17] structures exhibit magnetic characteristic under normal incident waves, they cannot maintain a similar magnetic response when the incident waves propagate along the lateral direction. Moreover, the magnitude modulation of a magnetic resonance is an important issue because resonance with sufficient strength to reach negative effective permeability is required in double negative materials, while this is not necessitated in the cloaking applications.

In this paper, we propose a metallic metamaterial composed of no-split rings and plates to explore its omnidirectional magnetic resonance transmission. The equivalent *LC* circuit model is used to investigate the dependence of magnetic resonance frequency on the geometric parameters. Additionally, we observe an elimination phenomenon of the magnetic resonance transmission through geometric modulation of the size of the plate component.

II. SIMULATION RESULTS

A. Omnidirectional magnetic resonance transmission

Figure 1 shows the unit cell of a metallic metamaterial composed of rings and plates as well as the propagation configurations of the incident electromagnetic wave. For simulation purpose, the sizes of the ring-plate unit cell are $L_x=L_z=3.8$ mm and $L_y=3.2$ mm. The edge length and width of the square ring are $a=3.0$ mm and $w=0.1$ mm, respectively. The in-plane and out-of-plane gaps, represented by g_x and g_y, are 0.1 and 0.4 mm, respectively. In addition, the metallic rings in 0.02 mm thickness (t) are placed in a host material of quartz with permittivity 3.78 and dielectric loss tangent 0.0001. In our numerical simulations based on the full-wave finite-element method, the simulation configuration has a dimension of $1\times1\times8$ units (i.e., one unit in the transverse xy plane and eight units in the electromagnetic propagation direction along the z axis). The polarized electric and magnetic

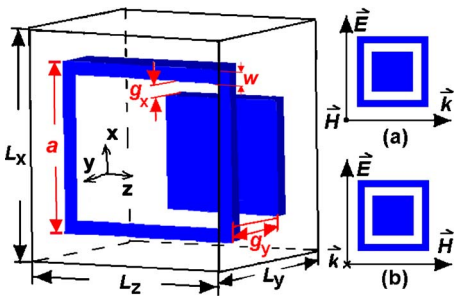

FIG. 1. (Color online) The left panel is a unit cell of the proposed metamaterial. The top and bottom of the right panel correspond to the lateral incidence case (a) and the normal incidence case (b), respectively. Note that the ring and plate are in different xz planes with an out-of-plane gap g_y in the y direction.

*Author to whom correspondence should be addressed. zgdong@seu.edu.cn

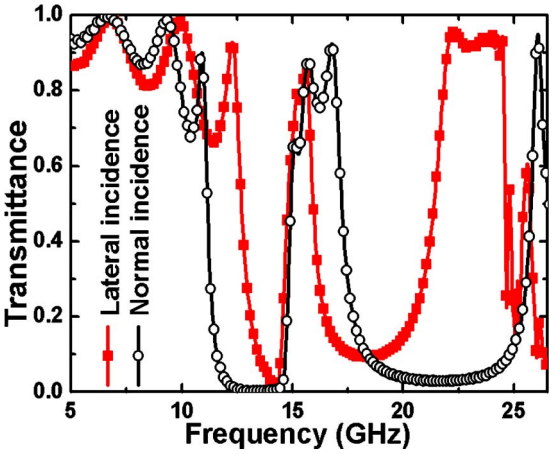

FIG. 2. (Color online) Transmittances of the ring-plate metamaterial.

fields of the incident wave are satisfied by applying the perfect electric and magnetic boundary conditions, respectively [18,19]. Taking into consideration the *xz* plane isotropy, there are three axial propagation cases that are independent of one another. The first one is that an electromagnetic wave propagates along the *z* axis with its polarized electric field in the *x* direction, called the lateral incidence case hereafter, as shown in the top of the right panel in Fig. 1. The second one presented in the bottom of the right panel in Fig. 1 is called the normal incidence case, since the wave vector of the incident field is perpendicular to the ring plane (i.e., the *xz* plane). These two cases have a common aspect of in-plane polarization of the electric field. The third case with electric field perpendicular to the ring plane is expected to exhibit no resonance in the corresponding frequency regime because neither the electric nor the magnetic field of the incident electromagnetic wave can induce current on the planar metallic faces. Therefore, the result of this incidence case is not considered in this paper.

The proposed metamaterial exhibits resonance transmission bands around 15.0 GHz for both the lateral and normal incidences (Fig. 2). It is interesting here that the normal incidence can produce a similar, except for a slightly wider, resonance transmission as compared with that of the lateral incidence case. Note that this result is obtained with structural symmetry of the ring-plate metamaterial about the direction of the polarized electric field (*x* axis), while for a split-ring metamaterial, contributed by Katsarakis *et al.*, the normal incidence can lead to similar magnetic response only when the mirror symmetry of the split ring with respect to the direction of the polarized electric field is broken, and hence electric coupling is introduced, by the splits of the rings [20]. As a matter of fact, the similar resonance transmissions between the two incidence cases in Fig. 2 imply an omnidirectional, but not completely, resonant response because the resonance transmission occurs for the in-plane polarization of the electric field. Additionally, it is noteworthy that, for the normal propagation configuration, it can yield sufficient response with only a one-unit layer in the propagation direction, which makes it rather convenient for fabrication purposes [9].

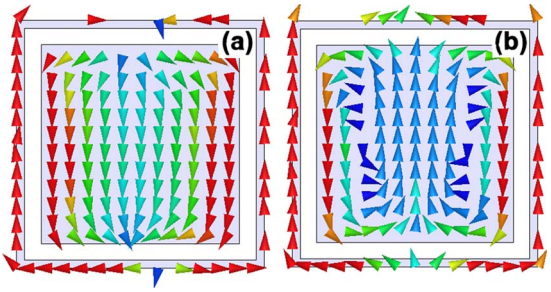

FIG. 3. (Color online) Induced current distributions on the planar metallic surfaces at magnetic resonance. (a) Lateral incidence. (b) Normal incidence.

As is well known, the electromagnetic property of a metamaterial is related to the engineered pattern rather than the constituent metal itself, and thus the shaped subwavelength elements are regarded as "meta-atoms." In such a sense, the induced current distribution associated with resonant magnetism should play a role that resembles the orbital motion or spin state of electrons in natural atoms and molecules. Therefore, it is conventional to investigate the induced current distributions for a better understanding of the electromagnetic responses in resonant metamaterials. In this work, to explore the origin of the resonance transmission, the induced current distributions at resonance frequency on the metallic surface are shown in Fig. 3, from which it is obvious that the antisymmetric mode of magnetic resonance [21,22] between the ring and plate are formed for both of the incidence cases (the left and right gaps can gather a large magnitude of magnetic field because of the antisymmetric mode). Generally, a magnetic resonance transmission band will not be formed unless the magnetic resonance occurs within the range of an otherwise electrical stop band. As for the ring-plate metamaterial, the electrical stop bands are from 12.2 to 22.1 GHz for the lateral incidence case and from 11.0 to 26.1 GHz for the normal incidence case (see Fig. 2), with the difference of these two frequency ranges mainly caused by the different propagation periodicities for the lateral and normal incidence cases, corresponding to L_z and L_y, respectively. As a result, the magnetic resonance around 15.0 GHz manifests as a resonance transmission rather than a stop band for both of the incidence cases. In addition, it is obvious that the induced currents on the plate surfaces are in different distributions for the two incidence cases. This discrepancy may contribute to the slightly wider resonance transmission for the normal incidence (see Fig. 2).

B. Resonance frequency dependence on the geometric configuration

In order to explore the dependence of the magnetic resonance frequency on the geometric configuration, the equivalent *LC* circuit model is used to calculate the magnetic resonance frequency $f_0=1/(2\pi\sqrt{L_{\text{eff}}C_{\text{eff}}})$, where the effective inductance L_{eff} as well as the effective capacitance C_{eff} are determined not only by the metallic shape but also by the distribution mode of the induced current at resonance. As for the ring-plate structure with the resonant current modes

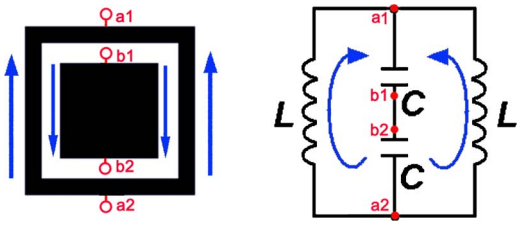

FIG. 4. (Color online) The equivalent *LC*-resonance circuit, associated with the induced current mode at magnetic resonance. The arrows illustrate the directions of the induced currents, and the points ($a1$, $a2$, $b1$, and $b2$) indicate the correspondence of the nodes between the metallic structure and its equivalent circuit.

shown in Fig. 3, an equivalent circuit constituted by inductors (L) and capacitors (C) is schematically drawn in Fig. 4 (without taking resistors into account), where L is proportional to the current circulating area [$\approx(2a-4w-2g_x)g$, see Fig. 3] and reversely proportional to the metallic thickness t, while C is proportional to the charge accumulation area [$\approx(a-2w-2g_x)t$, see Fig. 3] and reversely proportional to gap g in analogy to a parallel-plate capacitor [7–9,23]. Note that the gap g equals $\sqrt{g_x^2+g_y^2}$ and the total effective inductance L_{eff} equals $L/2$ because of the two parallel inductors, while the total effective capacitance C_{eff} equals $C/2$ because of the two series capacitors. Therefore, the inductance, capacitance, and magnetic resonance frequency can be estimated to be

$$L \approx \mu_0\mu(2a-4w-2g_x)g/t$$

and

$$C \approx \varepsilon_0\varepsilon(a-2w-2g_x)t/g.$$

Consequently,

$$f_0 = \frac{1}{2\pi\sqrt{L_{\text{eff}}C_{\text{eff}}}} = \frac{1}{\pi\sqrt{LC}} \approx \frac{1}{\pi\sqrt{\varepsilon_0\varepsilon\mu_0\mu}\sqrt{(2a-4w-2g_x)(a-2w-2g_x)}}.$$

For the case of w, $g_x \ll a$, the resonance frequency f_0 is mainly determined by a. The calculated resonance frequency from the formula for f_0 is 13.1 GHz, slightly smaller than the value of about 14.4 GHz from the numerical simulations shown in Fig. 2 (note that the resonance frequency in Fig. 2 should be located at the left side of the resonance transmission). The discrepancy is caused by both the approximation of the lumped elements and the unavoidable mutual inductance, which is not involved in Fig. 4. Furthermore, the formula for f_0 also indicates that it is independent of the out-of-plane gap g_y as well as the metallic thickness t. The g_y independence is confirmed by the results in Figs. 5(a) and 5(b) for the lateral and normal incidence case, respectively. The thickness independence of f_0 is also verified in our parametric simulations (not shown) and is consistent with the literature (see, for example, Refs. [7,16]).

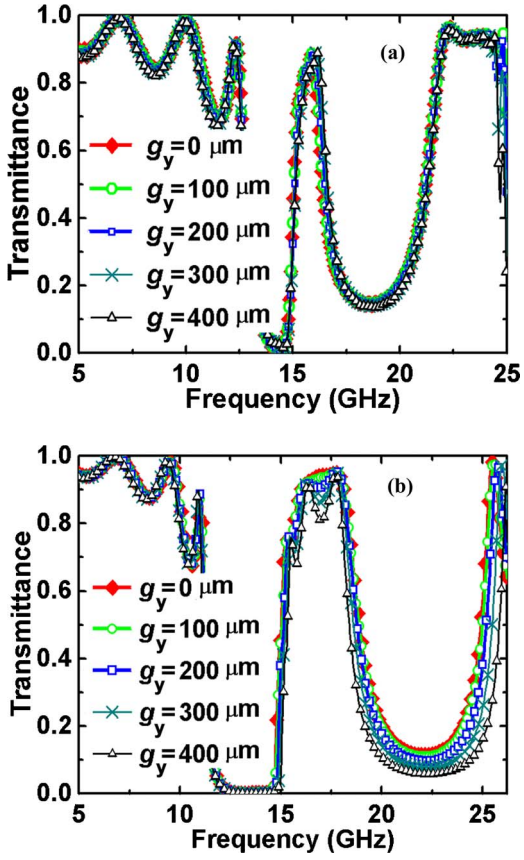

FIG. 5. (Color online) The dependence of magnetic resonance transmission on the out-of-plane gap g_y. (a) Lateral incidence case. (b) Normal incidence case.

C. Elimination of magnetic resonance transmission

As is known, magnetic resonance with sufficient magnitude (i.e., negative effective permeability) is necessary to get a high resonance transmission within an otherwise electrically formed stop band. In this section, we investigate an elimination phenomenon of the magnetic resonance transmission by tuning the size of the plate component, which implies an approach of magnitude modulation of magnetic resonance transmission.

Figures 6(a) and 6(b) show the transmittance dependence on the in-plane gap g_x at the lateral and normal incidence case, respectively. The variation of g_x is obtained by modifying the size of the plate, thus the negative values of g_x mean larger sizes of the plate than the inner separation of the ring (i.e., plate size $>a-2w$). It is obvious that, for both of the incidence cases, the transmission magnitude of the magnetic resonance is more and more suppressed with the plate size (i.e., decreasing the value of g_x). Roughly, the positive values of g_x result in high transmissions of magnetic resonance, while the negative values of g_x lead to suppressions, or even eliminations of the magnetic resonance transmission. It is believed that transmission elimination of magnetic resonance implies the vanishing of strong magnetic activity. To clarify the dependence of the magnitude of magnetic resonance transmission on the size of the metallic plate, we can resort to the quality factor [$Q=(1/2R)\sqrt{L_{\text{eff}}/C_{\text{eff}}}$] in the view-

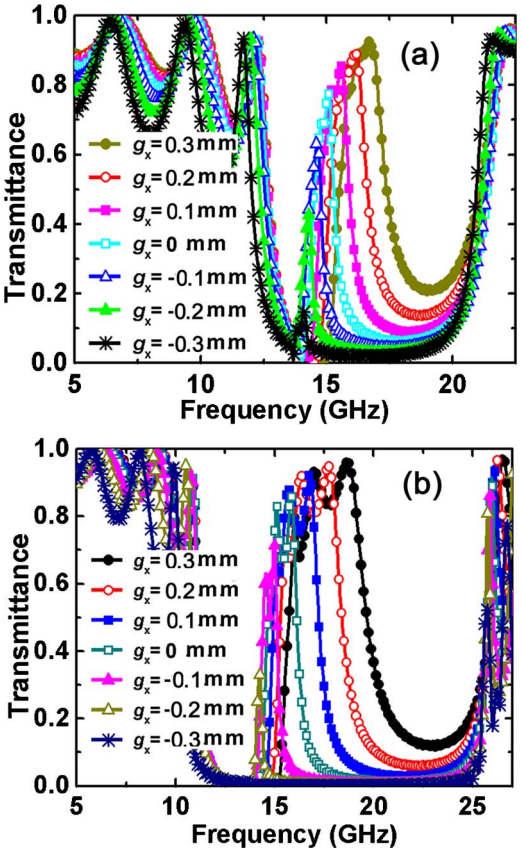

FIG. 6. (Color online) The dependence of magnetic resonance transmission on the in-plane gap g_x. (a) Lateral incidence case. (b) Normal incidence case.

point of the equivalent *LC* circuit model. It was recently studied by Zhou *et al.* [24] that increasing the *Q* factor is an efficient way to reduce losses and, hence, to enhance the left-handed transmission (magnetic resonance transmission). In this work, by reducing the size of the metallic plate (increasing g_x), L_{eff} increases because of the increased circulating area of induced current, and C_{eff} decreases because of the reduced charge accumulation area as well as the increased gap g (see the deduced formula in Sec. II B). Consequently, the *Q* factor increases with g_x, which leads to an enhanced magnitude of the magnetic resonance transmission, as the simulation results show in Figs. 6(a) and 6(b).

III. CONCLUSIONS

We have investigated numerically a metallic metamaterial composed of rings and plates. First, the omnidirectional magnetic resonance transmission is formed within the frequency range of an otherwise electrical stop band, which resembles the response of a double negative material in the viewpoint of the left-handed electromagnetic mechanism [25–27]. However, the effective permittivity and permeability are not retrieved for the ring-plate composite structure, since the magnetic resonance wavelength in the host quartz (about 10 mm) is smaller than three times the unit sizes and thus the effective medium theory might not be applicable. Second, the controllability of the magnetic resonance, in terms of the magnitude suppression of the resonance transmission, is observed by modulation of the size of the metallic plate. This result can be interpreted by the *Q* factor according to the equivalent *LC* circuit model.

ACKNOWLEDGMENTS

This work was supported by the State Key Program for Basic Research of China (Grants No. 2004CB619003, No. 2006CB921804, and No. 2009CB930501) and the National Natural Science Foundation of China (Grants No. 10534020, No. 10604029, No. 10704036, No. 10747116, No. 60578034, and No. 10874081). M.-X.X. also acknowledges the support from the National Science Foundation of Jiangsu Province of China (Grant No. BK2007118), Research Fund for the Doctoral Program of Higher Education of China (Grant No. 20070286037).

[1] D. R. Smith, J. B. Pendry, and M. C. K. Wiltshire, Science **305**, 788 (2004).
[2] X. Zhang and Z. Liu, Nature Mater. **7**, 435 (2008).
[3] J. B. Pendry, D. Schurig, and D. R. Smith, Science **312**, 1780 (2006).
[4] C. Enkrich, M. Wegener, S. Linden, S. Burger, L. Zschiedrich, F. Schmidt, J. F. Zhou, T. Koschny, and C. M. Soukoulis, Phys. Rev. Lett. **95**, 203901 (2005).
[5] B. D. F. Casse, H. O. Moser, J. W. Lee, M. Bahou, S. Inglis, and L. K. Jian, Appl. Phys. Lett. **90**, 254106 (2007).
[6] H. Liu, D. A. Genov, D. M. Wu, Y. M. Liu, J. M. Steele, C. Sun, S. N. Zhu, and X. Zhang, Phys. Rev. Lett. **97**, 243902 (2006).
[7] J. Zhou, E. N. Economon, Th. Koschny, and C. M. Soukoulis, Opt. Lett. **31**, 3620 (2006).
[8] S. Tretyakov, Metamaterials **1**, 40 (2007).
[9] M. Kafesaki, I. Tsiapa, N. Katsarakis, Th. Koschny, C. M. Soukoulis, and E. N. Economou, Phys. Rev. B **75**, 235114 (2007).
[10] S. Linden, C. Enkrich, M. Wegener, J. Zhou, T. Koschny, and C. M. Soukoulis, Science **306**, 1351 (2004).
[11] J. Zhou, Th. Koschny, L. Zhang, G. Tuttle, and C. M. Soukoulis, Appl. Phys. Lett. **88**, 221103 (2006).
[12] C. Enkrich, F. Perez-Willard, D. Gerthsen, J. Zhou, Th. Koschny, C. M. Soukoulis, M. Wegener, and S. Linden, Adv. Mater. (Weinheim, Ger.) **17**, 2547 (2005).
[13] S. Zhang, W. Fan, N. C. Panoiu, K. J. Malloy, R. M. Osgood, and S. R. J. Brueck, Phys. Rev. Lett. **95**, 137404 (2005).
[14] V. D. Lam, J. B. Kim, S. J. Lee, and Y. P. Lee, J. Appl. Phys. **103**, 033107 (2008).
[15] K. Aydin, Z. Li, L. Sahin, and E. Ozbay, Opt. Express **16**, 8835 (2008).
[16] J. Zhou, L. Zhang, G. Tuttle, Th. Koschny, and C. M. Soukoulis, Phys. Rev. B **73**, 041101(R) (2006).

[17] V. M. Shalaev, W. Cai, U. K. Chettiar, H.-K. Yuan, A. K. Sarychev, V. P. Drachev, and A. V. Kildishev, Opt. Lett. **30**, 3356 (2005).
[18] Z.-G. Dong, M. X. Xu, S. Y. Lei, H. Liu, T. Li, F. M. Wang, and S. N. Zhu, Appl. Phys. Lett. **92**, 064101 (2008).
[19] F. M. Wang, H. Liu, T. Li, Z. G. Dong, S. N. Zhu, and X. Zhang, Phys. Rev. E **75**, 016604 (2007).
[20] N. Katsarakis, T. Koschny, M. Kafesaki, E. N. Economou, and C. M. Soukoulis, Appl. Phys. Lett. **84**, 2943 (2004).
[21] A. N. Grigorenko, A. K. Geim, H. F. Gleeson, Y. Zhang, A. A. Firsov, I. Y. Khrushchev, and J. Petrovic, Nature **438**, 335 (2005).
[22] V. M. Shalaev, Nat. Photonics **1**, 41 (2007).
[23] K. Busch, G. V. Freymann, S. Linden, S. F. Mingaleev, L. Tkeshelashvili, and M. Wegener, Phys. Rep. **444**, 101 (2007).
[24] J. Zhou, Th. Koschny, and C. M. Soukoulis, Opt. Express **16**, 11147 (2008).
[25] J. B. Pendry and D. R. Smith, Phys. Today **57** (6), 37 (2004).
[26] D. R. Smith, J. B. Pendry, and M. C. K. Wiltshire, Science **305**, 788 (2004).
[27] C. M. Soukoulis, S. Linden, and M. Wegener, Science **315**, 47 (2007).